Thermoelastic analysis of FGM beam using meshless weighted least-square method

Zhou H.M.

School of Mechanical and Power Engineering, Henan Polytechnic University, JiaoZuo, China

Corresponding author: zhm_1979@163.com

Abstract

The paper analyzes the thermoelastic problem of the FGM beam using meshless weighted least-square method (MWLS). The MWLS as a meshless method is fully independent of mesh, and a discrete function is used to construct a series of linear equations, which avoided the troublesome task of numerical integration. The effectiveness and accuracy of the approach are illustrated by a clamped-clamped FGM beam which is subjected with interior heat source. The volume fraction of FGM beam is assumed to be given by a simple power law distribution. Material properties of the FGM beam are assumed to be temperature independent and calculated by Mori-Tanaka method. The results shows that a good agreement is achieved between the proposed meshless method and commercial COMSOL Multiphysics.

Keywords: thermoelastic analysis; FGM beam; Meshless weighted least-square method.

1 Introduction

FGM object can resist high temperatures and are profient in reducing the thermal stress, and have received a considerable attention from the researchers [1]. Various numerical techniques, such as the finite difference method [2], finite element method [3-4], boundary element method [5] or more recently developed meshless methods[6-11], have been developed for analyzing these thermoelastic and heat conduction problems. Because of the complexity of the relevant governing equation, analytical solutions are usually difficult to obtain for those arbitrary geometry and complex boundary conditions. Compared with FEM, FDM and BEM, the meshless methods is associated with a class of numerical techniques that approximate a given differential equation or a set of differential equations using global interpolations on the discrete nodes or background mesh, exhibiting the advantages of avoiding mesh generation, simple data preparation, easy post-processing and so on.

Liu and Gu [12] introduced meshless methods and their programming, such as the element-free Galerkin (EFG) method, the hp-clouds method, the meshless local Petrov-Galerkin (MLPG) method, meshless Galerkin method using radial basis functions, the least-square method and meshless point collocation method. The main advantage of the MLPG method [6-7] compared with regular Galerkin-based methods is that no background mesh is used to evaluate various integrals appearing in the local weak formulation of problem, but it requires a high-order quadrature rule to obtain converged results and thus needs much more computational effort in terms of CPU time than that for the FEM. Katsikadelis [10]

employed the meshless analog equation method to solve the 2D elastostatic problem for inhomogeneous anisotropic. A meshless algorithm of fundamental solution coupling with radial basis functions based on analog equation theory was proposed to simulate the static thermal stress distribution in 2D FGMs [11]. Bhavani etc.[13] solved thermoelastic equilibrium equations for a functionally graded beam to obtain the axial stress distribution. Sohn and Kim[14] analysized static and dynamic stabilities of FG panels which are subjected to thermal and aerodynamic loads.

Zhou etc. presented steady-state[15] and transient-state[16] heat conduction analysis of heterogeneous material using the meshless weighted least-square method. In this paper the pure meshless method (MWLS) was then extended to solve problems of thermoelastic analysis for the FGM beam with interior heat source. The volume fractions of constituent materials composing the FGM beam are assumed to be given by a simple power law distribution. Material properties of the FGM are obtained by Mori-Tanaka method. The paper is divided as follows: in section 2, we give problem description and MWLS analysis about the thermoelastic problem. In order to demonstrate the efficiency and accuracy of the proposed method, numerical implementation is given in section 3. The last section includes some conclusions.

2. MWLS analysis of the thermoelastic problem

The basis of MWLS analysis is described in this section. The shape functions in MWLS analysis is a moving least-squares approximation scheme which is originally developed for the smooth interpolation of irregularly distributed data.

2.1 The Moving Least-square (MLS) approximation scheme

The local approximate function of $f(\boldsymbol{x})$ is expressed as

$$f(x) \approx f^h(\boldsymbol{x}) = N_I(\boldsymbol{x}) f_I = \boldsymbol{p}^T(\boldsymbol{x})\boldsymbol{a}(\boldsymbol{x}) \tag{1}$$

Where $\boldsymbol{p}^T(\boldsymbol{x})$ is the basis function and the quadratic basis $\boldsymbol{p}^T(\boldsymbol{x}) = \{1, x, y, x^2, xy, y^2\}$ is used in this paper; $\boldsymbol{a}(\boldsymbol{x})$ is the coefficient, which is determined by minimizing a functional of weighted residual

$$J = \sum_{I=1}^{N} \omega_I(\boldsymbol{x})[f^h(\boldsymbol{x}, \boldsymbol{x}_I) - f(\boldsymbol{x}_I)]^2 = \sum_{I=1}^{N} \omega_I(\boldsymbol{x})[\boldsymbol{p}^T(\boldsymbol{x})\boldsymbol{a}(\boldsymbol{x}) - f(\boldsymbol{x}_I)]^2 \tag{2}$$

The minimum value of J may be obtained through differentiating with respect to $\boldsymbol{a}(\boldsymbol{x})$

$$\frac{\partial J}{\partial a_j(\boldsymbol{x})} = 2\sum_{I=1}^{N} \omega_I(\boldsymbol{x})[\sum_{i=1}^{m} p_i(\boldsymbol{x}_I) a_i(\boldsymbol{x}) - f_I] p_j(\boldsymbol{x}_I) = 0 \qquad j=1,2,\ldots,m \tag{3}$$

Where $\boldsymbol{x}_I$ are the positions of the N nodes, f_I is the nodal parameter of the field variable at node I. $\omega_I(\boldsymbol{x})$ is the weighting function and usually a compactly supported function that is

only nonzero in a small neighborhood called the "support domain" of node $\boldsymbol{x}_I$. The gauss function is used in this paper.

$$\omega(r)=\begin{cases}(\exp(-r^2\beta^2)-\exp(-\beta^2))/(1-\exp(-\beta^2)) & r\le 1\\ 0 & r>1\end{cases} \qquad (4)$$
$$r=\left\|\boldsymbol{x}-\boldsymbol{x}_I\right\|/d_{mI}$$

Solving $\boldsymbol{N}(\boldsymbol{x})$ from Eq.(1) and Eq.(3), the shape function is given by:

$$\boldsymbol{N}(\boldsymbol{x})=\boldsymbol{p}^T(\boldsymbol{x})\boldsymbol{A}^{-1}(\boldsymbol{x})\boldsymbol{B}(\boldsymbol{x}) \qquad (5)$$

Where the matrices $\boldsymbol{A}(\boldsymbol{x})$ and $\boldsymbol{B}(\boldsymbol{x})$ are defined as

$$\begin{cases}\boldsymbol{A}(\boldsymbol{x})\boldsymbol{a}(\boldsymbol{x})=\boldsymbol{B}(\boldsymbol{x})f\\ \boldsymbol{A}(\boldsymbol{x})=\sum_{I=1}^{N}\omega_I(\boldsymbol{x})\boldsymbol{p}(\boldsymbol{x}_I)\boldsymbol{p}^T(\boldsymbol{x}_I)\\ \boldsymbol{B}(\boldsymbol{x})=[\omega_1(\boldsymbol{x})p(\boldsymbol{x}_1)\quad \omega_2(\boldsymbol{x})p(\boldsymbol{x}_2)\quad \ldots\quad \omega_N(\boldsymbol{x})p(\boldsymbol{x}_N)]\end{cases} \qquad (6)$$

In Eq.(4) the radius of the circular support domain, d_{mI}, is chosen to make the matrix $\boldsymbol{A}(\boldsymbol{x})$ nonsingular everywhere in the domain, i.e., the support domain must have enough neighborhood nodes. Through finding the kk^{th} nearest points of the evaluation point $\boldsymbol{x}$, the smallest support domain including these points can be obtained. The selection of kk is to compare some numerical examples with their analytical solution in Zhou et al.[16].

2.2 Thermoelastic analysis of FGM object

Consider the 2D FGM anisotropic linear elastic body occupying the domain Ω with boundary Γ of the xy plane. The governing equation and boundary condition are as follows,

$$\sigma_{ij,j}=0 \quad in \quad \Omega \qquad (7)$$

$$\begin{aligned}&\text{stress boundary condition: } \sigma_{ij}n_j-\overline{t}_i=0 \quad \text{on} \quad \Gamma_t\\ &\text{displacement boundary condition: } u_i=\overline{u}_i \quad \text{on} \quad \Gamma_u\end{aligned} \qquad (8)$$

where σ_{ij} is the components of the Cauchy stress tensor. A comma followed by index j denotes the partial differentiation with respect to coordinate x_j of a material point. u_i are the displacement components, and $\overline{u}_i$ are the prescribed displacements on Γ_u and $\overline{t}_i$ are the given tractions on Γ_t where Γ_u and Γ_t are the complementary parts of the boundary Γ.

$$\sigma_{ij,j}(\boldsymbol{x}_k)=0 \qquad \boldsymbol{x}_k\in\Omega, i,j=1,2; k=1,2,\ldots,N_\Omega \qquad (9)$$
$$\sigma_{ij}(\boldsymbol{x}_k)n_j=\overline{t}_i(\boldsymbol{x}_k) \qquad \boldsymbol{x}_k\in\Gamma_t, i,j=1,2; k=1,2,\ldots,N_t \qquad (10)$$
$$u_i(\boldsymbol{x}_k)=\overline{u}_i(\boldsymbol{x}_k) \qquad \boldsymbol{x}_k\in\Gamma_u, i=1,2; k=1,2,\ldots,N_u \qquad (11)$$

Substituting the approximate shape function $\boldsymbol{f}$ of Eq.(9~11) into Eq.(1),

$$\sum_{I=1}^{N}\boldsymbol{H}_I(x_k)\boldsymbol{f}_I=0 \qquad x_k\in\Omega, k=1,2,\ldots,N_\Omega \qquad (12)$$

$$\sum_{I=1}^{N} \boldsymbol{Q}_I(x_k)\boldsymbol{f}_I = \overline{\boldsymbol{t}}_k \qquad x_k \in \Gamma_t, k = 1,2,...,N_t \tag{13}$$

$$\sum_{I=1}^{N} \boldsymbol{N}_I(x_k)\boldsymbol{f}_I = \overline{\boldsymbol{u}}_k \qquad x_k \in \Gamma_u, k = 1,2,...,N_u \tag{14}$$

Where

$$\boldsymbol{H}_I(x_k) = \frac{E}{1-\upsilon^2}\begin{bmatrix} \dfrac{\partial^2 N_I(x_k)}{\partial x^2} + \dfrac{1-\upsilon}{2}\dfrac{\partial^2 N_I(x_k)}{\partial y^2} & \dfrac{1+\upsilon}{2}\dfrac{\partial^2 N_I(x_k)}{\partial x \partial y} \\ \dfrac{1+\upsilon}{2}\dfrac{\partial^2 N_I(x_k)}{\partial x \partial y} & \dfrac{\partial^2 N_I(x_k)}{\partial y^2} + \dfrac{1-\upsilon}{2}\dfrac{\partial^2 N_I(x_k)}{\partial x^2} \end{bmatrix} \tag{15}$$

$$\boldsymbol{Q}_I(x_k) = \frac{E}{1-\upsilon^2}\begin{bmatrix} l\dfrac{\partial N_I(x_k)}{\partial x} + m\dfrac{1-\upsilon}{2}\dfrac{\partial N_I(x_k)}{\partial y} & l\upsilon\dfrac{\partial N_I(x_k)}{\partial y} + m\dfrac{1-\upsilon}{2}\dfrac{\partial N_I(x_k)}{\partial x} \\ m\upsilon\dfrac{\partial N_I(x_k)}{\partial x} + l\dfrac{1-\upsilon}{2}\dfrac{\partial N_I(x_k)}{\partial y} & m\dfrac{\partial N_I(x_k)}{\partial y} + l\dfrac{1-\upsilon}{2}\dfrac{\partial N_I(x_k)}{\partial x} \end{bmatrix} \tag{16}$$

$$\boldsymbol{N}_I = \begin{bmatrix} \boldsymbol{N}_I(x_k) & 0 \\ 0 & \boldsymbol{N}_I(x_k) \end{bmatrix}, \quad \boldsymbol{f}_I = \begin{bmatrix} f_{1I} \\ f_{2I} \end{bmatrix}, \overline{\boldsymbol{t}}_k = \begin{bmatrix} \overline{t}_1(x_k) \\ \overline{t}_2(x_k) \end{bmatrix}, \quad \overline{\boldsymbol{u}}_k = \begin{bmatrix} \overline{u}_1(x_k) \\ \overline{u}_2(x_k) \end{bmatrix} \tag{17}$$

Where, $l = \cos(No, x)$, $m = \cos(No, y)$, No is the nomal vector of any point. $\boldsymbol{H}$,$\boldsymbol{Q}$ and $\boldsymbol{N}$ are the shape function.

Substituting the approximate function $\boldsymbol{f}$ of Eq.(7~8) into Eq.(1), the residuals are minimized in a least-squares manner,

$$\Pi = \int_{\Omega} \sigma_{ij,j}\sigma_{ik,k}\,d\Omega + \int_{\Gamma u} (u_i - \overline{u}_i)(u_i - \overline{u}_i)\,d\Gamma u + \int_{\Gamma t} (\sigma_{ij}n_j - \overline{t}_i)(\sigma_{ij}n_j - \overline{t}_i)\,d\Gamma t \tag{18}$$

The system equations of the MWLS method for solving thermoelastic problem are obtained as

$$\boldsymbol{K}\boldsymbol{d} = \boldsymbol{P} \tag{19}$$

Where

$$\boldsymbol{K} = \sum_{s=1}^{N} \boldsymbol{H}^T(x_s)\boldsymbol{H}(x_s) + \sum_{s=1}^{N_u} \boldsymbol{N}^T(x_s)\boldsymbol{N}(x_s) + \sum_{s=1}^{N_t} \boldsymbol{Q}^T(x_s)\boldsymbol{Q}(x_s) \tag{20}$$

$$\boldsymbol{P} = -\sum_{s=1}^{N} \boldsymbol{H}^T(x_s)\overline{f}_s + \sum_{s=1}^{N_u} \boldsymbol{N}^T(x_s)\overline{u}_s + \sum_{s=1}^{N_t} \boldsymbol{Q}^T(x_s)\overline{t}_s \tag{21}$$

Where, $\boldsymbol{H}$,$\boldsymbol{Q}$ and $\boldsymbol{N}$ are obtained by Eq.(15~17), $\boldsymbol{d}$ denotes the displacement of x,y. $\boldsymbol{D}$ is the stiffness matrix for a linearly elastic, isotropic 2-D solid.

$$\boldsymbol{\sigma} = \boldsymbol{D}\boldsymbol{\varepsilon} - \boldsymbol{\beta}\theta \tag{22}$$

$$\boldsymbol{D} = \frac{\overline{E}(x)}{1-\overline{\upsilon}(x)^2}\begin{bmatrix} 1 & \overline{\upsilon}(x) & 0 \\ \overline{\upsilon}(x) & 1 & 0 \\ 0 & 0 & (1-\overline{\upsilon}(x))/2 \end{bmatrix} \tag{23}$$

in which $\bar{E} = E$; $\bar{\upsilon} = \upsilon$; $\boldsymbol{\beta} = \dfrac{\alpha E}{1-\upsilon}\begin{Bmatrix}1\\1\\0\end{Bmatrix}$, for plane stress with E、γ and α denoting the Young's modulus, Poisson's ratio, and coefficient of thermal expansion, respectively, and $\bar{E} = \dfrac{E}{1-\upsilon^2}$; $\bar{\upsilon} = \dfrac{\upsilon}{1-\upsilon}$; $\boldsymbol{\beta} = \dfrac{\alpha E}{1-2\upsilon}\begin{Bmatrix}1\\1\\0\end{Bmatrix}$ for plane stain.

2.3 material properties

There are two methods to describe the variance of the material properties. One is to use the specific functions for all kinds of material properties. The other is to employ the specific functions of volume fraction of FGM objects. In this paper, relevant material properties at the discrete points are determined based on Mori-Tanaka model [17]. It is the modified rule of mixtures and the effective material properties can be determined using the following relation,

$$k = k_1 + \frac{3k_1V_2(k_2 - k_1)}{3k_1 + V_1(k_2 - k_1)} \tag{24}$$

$$E = E_1 + \frac{V_2(3E_1 + 4\mu_1)(E_2 - E_1)}{3(1-V_2)(E_2 - E_1) + 3E_1 + 4\mu_1} \tag{25}$$

$$\mu = \mu_1 + \frac{V_2(\mu_1 + f_1)(\mu_2 - \mu_1)}{(1-V_2)(\mu_2 - \mu_1) + \mu_1 + f_1} \tag{26}$$

$$\alpha = \alpha_1 + \frac{E_2(E_1 - E)(\alpha_2 - \alpha_1)}{E(E_1 - E_2)} \tag{27}$$

Where, $E_1 = \dfrac{P_1}{3(1-2\upsilon_1)}$; $E_2 = \dfrac{P_2}{3(1-2\upsilon_2)}$; $\mu_1 = \dfrac{P_1}{2(1+\upsilon_1)}$; $\mu_2 = \dfrac{P_2}{2(1+\upsilon_2)}$; $f_1 = \dfrac{\mu_1(9E_1 + 8\mu_1)}{6(E_1 + 2\mu_1)}$, P may be modulus of elasticity, Poisson's ratio υ, bulk modulus E, shear modulus μ, thermal conductivity k, volume fraction V and coefficient of thermal expansion α.

3 Numerical results and discussions

A clamped-clamped FGM beam is shown in Figure 1, length L=1000mm, width D=500mm and thickness H=100mm, k1=233W/mK, k2=65W/mK, E1=7e10Pa, E2=4.27e11Pa, v1=0.3, v2=0.17, alfa1=2.34e-5/K, alfa2=4.3e-6/K, Q=5e5W/m3, the spatial variation of the volume fraction of material 1 is taken to be a power law distribution in the y-direction as V=(y/D)^a.

The beam is assumed to be in a state of plane strain normal to the xy plane, and the design region is discretized as 31×15. The effective material properties are determined by the Mori-Tanaka scheme. In order to verify our method, we do some compararions between MWLS and the commercial COMSOL Multiphysics for uniform material (a=0), relevant

results listed in Table 1. The results obtained with the two methods are in good agreement in Table 1. The maximum temperature 361.8K is in the center (0.5,0.25) of the beam.

For a=2, we analyzed the thermoelastic problem and heat conduction problem using MWLS, details of heat conduction analysis using MWLS can be found in Zhou et al.[15]. Temperature field distribution, x-displacement and y-dispalcement are shown in Figure2, Figure3 and Figure4, respectively. Figure 2 indicates that the maximum temperature 425.6K is higher that the uniform material, in the Cartesian Coordinates (0.5,0.179) of the beam. Figure 3 and Figure 4 show that, when subjected to temperature rise, the beam expands, the maximum y-displacement is located at the top middle of the beam. To make a comparison, we do thermoelastic analysis and obtain thermal stresses in the neutral axis of the beam among a=0,a=2 and a=3, as shown in Figure5. In Figure5 (a) and (c), the volume fraction of material 1 is gradually decreased from a=0 to a=3, the σx and σy stesses are be in an upward trend. The maximum thermal stress always occurred in the vicinity of neutral axis of the beam from Figure5 (a,c,d). The results also agreed well with the presented elasticity solutions of Ref [13].

Table 1. Compararion of MWLS method and COMSOL Multiphysics

method	Temperature/K		X displacement /mm		Y displacement/mm	
	maximum	minimum	maximum	minimum	maximum	minimum
MWLS	361.8	300	.596	-.873	2.7	-2.6
COMSOL Multiphysics	361.1	300	.639	-.639	3.81	-3.81

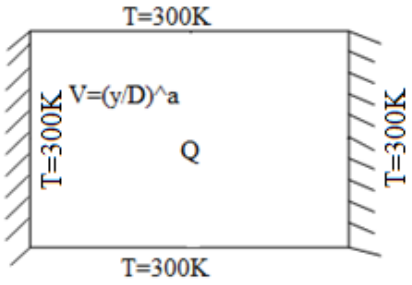

Figure1. Initial condition

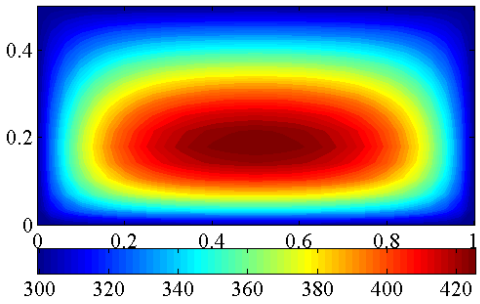

Figure 2. Distribution of temperature field

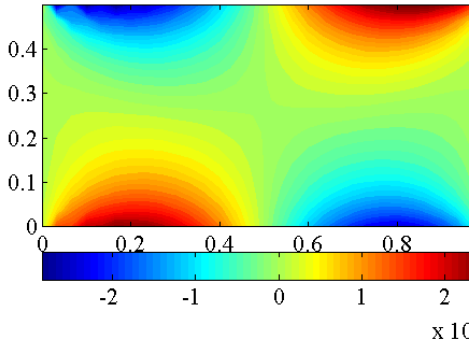

Figure 3. x-displacement/m

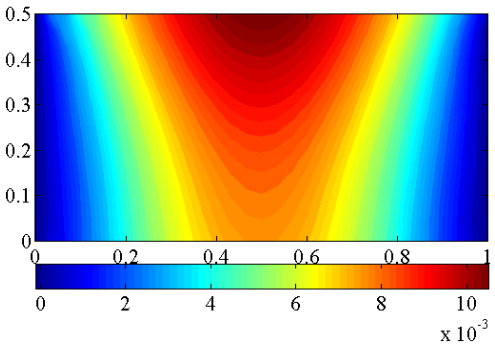

Figure 4. y-displacement /m

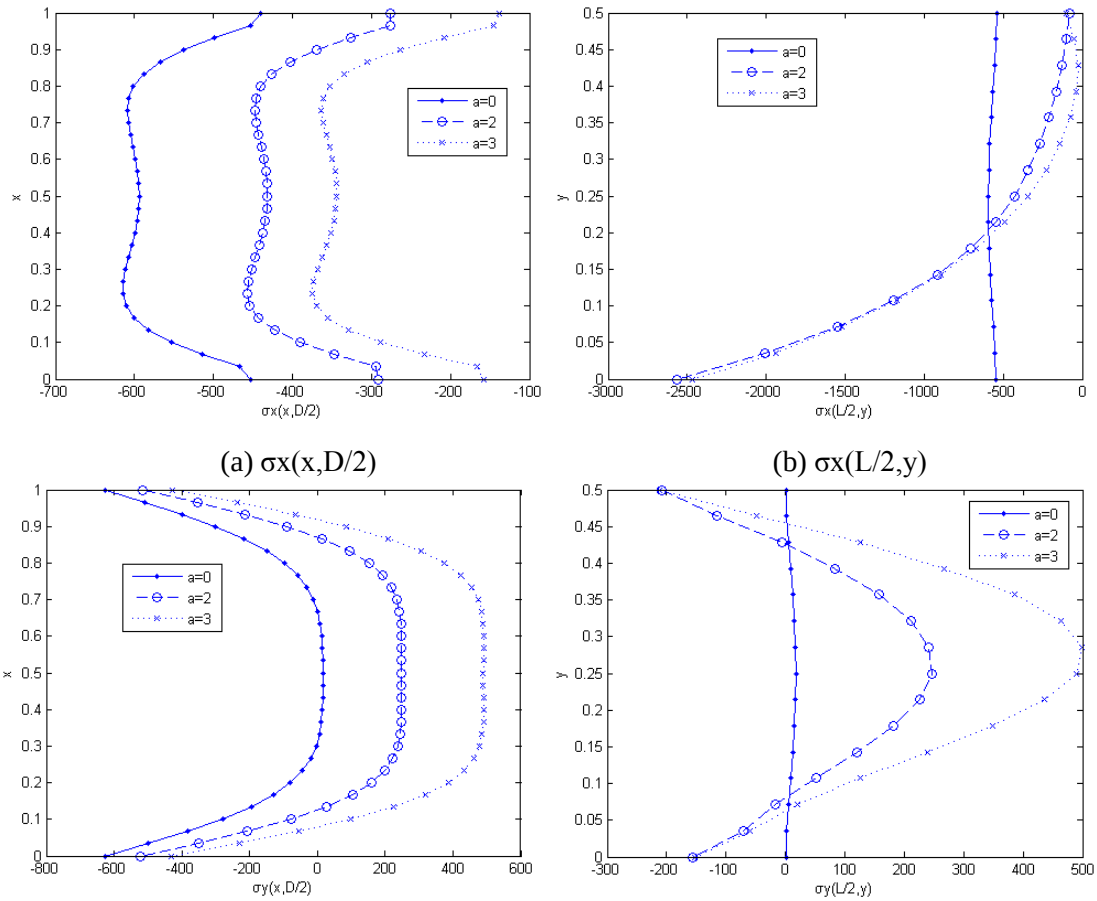

(a) σx(x,D/2) (b) σx(L/2,y)

(c) σy(x,D/2) (d) σy(L/2,y)

Figure 5. Stress results compararion of thermoelastic analysis among a=0,a=2 and a=3

4 Conlusion

In this paper, a noval thermoelastic analysis of FGM beam based on MWLS method was presented. We do thermoelastic and heat conduction analysis aimed at a clamped-clamped thick beam which is subjected with interior heat source. The FGM beam is assumed to be given by a simple power law distribution. Material properties of the FGM beam are obtained by Mori-Tanaka method. Through compared with the commercial software, it verified the effectiveness and accuracy. We also listed the compararion of thermal stresses with the varation of power law index. The present method of analysis will be also useful in the design and optimization of FGM objects.

Acknowledgements

The work described in this paper was supported by a grant from the National Natural Science Foundation of China (Projects No.51505131), the Fundamental Research Funds for the Universities of Henan Province and a doctor fund (No. B2013-032) and Program for Innovative Research Team (No.T2017-3) of Henan Polytechnic University. The correlative members of the projects are hereby acknowledged.

References

[1] K.Swaminathan, D.M.Sangeetha. (2017) Thermal analysis of FGM plates – A critical review of various modeling techniques and solution methods. Composite Structures 160, 43-60.

[2] Sergio Turteltaub. (2002) Optimal control and optimization of functionally graded materials for thermomechanical processes. International Journal of Solids and Structures 39, 3175-3197.

[3] Kou X.Y., Tan S.T. (2007) A systematic approach for Integrated Computer-Aided Design and Finite Element Analysis of Functionally-Graded-Material objects. Materials and Design 28, 2549-2565.

[4] M.Lezgy-Nazargah. (2015) Fully coupled thermo-mechanical analysis of bi-directional FGM beams using NURBS isogeometric finite element approach. Aerospace Science and Technology 45, 154-164.

[5] Alok Sutradhar, Glaucio H.Paulino. (2004) The simple boundary element method for transient heat conduction in functionally graded materials. Comput.Methods Appl. Mech. Engrg.193, 4511-4539.

[6] Ching H.K.,Chen J.K. (2007) Thermal stress analysis of Functionally Graded composites with temperature-dependent material properties. Journal of mechanics of materials and structures 2,633-653.

[7] H.K.Ching, S.C.Yen. (2005) Meshless local Petrov-Galerkin analysis for 2D functionally graded elastic solids under mechanical and thermal loads. Composites:Part B 36, 223-240.

[8] Hui wang, Qing-Hua Qin. (2008) Meshless approach for thermo-mechanical analysis of functionally graded materials. Engineering Analysis with Boundary Elements 32, 704-712.

[9] Andrew J.Goupee, Senthil S.Vel. (2006) Two-dimensional optimization of material composition of functionally graded materials using meshless analyses and a genetic algorithm. Comput. Mehtods Appl. Mech. Engrg.195, 5926-5948.

[10] John T.Katsikadelis. (2008) The 2D elastostatic problem in inhomogeneous anisotropic bodies by the meshless analog equation method (MAEM). Engineering Analysis with Boundary Elements.32, 997-1005.

[11] D.F.Gilhooley, J.R.Xiao, R.C.Batra. etc. (2008) Two-dimensional stress analysis of functionally graded solids using the MLPG method with radial basis functions. Computational Materials Science 41, 467-481.

[12] Liu G.R, Gu Y.T. (2005) An introduction to meshfree methods and their programming. Springer, Berlin.

[13] Bhavani V.Sankar, Jerome T.Tzeng. (2002) Thermal stresses in Functionally Graded Beams. AIAA Journal. Vol.40,1228-1232.

[14] K.J.Sohn, J.H.Kim. (2008) Structural stability of functionally graded panels subjected to aero-thermal loads. Composite Structures 82, 317-325.

[15] Zhou H.M., Liu Z.G. and Lu B.H. (2010) Heat conduction analysis of heterogeneous objects based on multi-color distance field. Mater Design 31, 3331-3338.

[16] Zhou H.M., Zhou W.H., Qin G. etc. (2017) Transient heat conduction analysis for distance-field-based irregular geometries using the meshless weighted least-square method. Numerical Heat Transfer, Part B:Fundamentals 71, 456-466.

[17] X.Peng, N.Hu, H.Zheng, H.Fukunaga. (2009) Evaluation of mechanical properties of particulate composites with a combined self-consistent and Mori–Tanaka approach. Mechanics of Materials 41, 1288-1297.